Available online at www.sciencedirect.com
ScienceDirect
Materials Research Bulletin 43 (2008) 1057–1065
Materials Research Bulletin
www.elsevier.com/locate/matresbu

Luminescent properties of $Sr_2P_2O_7$:Eu,Mn phosphor under near UV excitation

Shi Ye [a], Zhong-Shi Liu [a], Jia-Guo Wang [b], Xi-Ping Jing [a,*]

[a] *Beijing National Laboratory for Molecular Sciences, State Key Laboratory of Rare Earth Materials & Applications, College of Chemistry and Molecular Engineering, Peking University, Beijing 100871, PR China*
[b] *College of Chemistry and Materials Science, Wenzhou University, Wenzhou 325027, PR China*

Received 23 March 2007; received in revised form 13 July 2007; accepted 26 July 2007
Available online 2 August 2007

Abstract

The phosphors in the system $Sr_{2-x-y}P_2O_7$:xEu^{2+},yMn^{2+} were synthesized by solid-state reactions and their photoluminescence properties were investigated. These phosphors have strong absorption in the near UV region, which is suitable for excitation of ultraviolet light emitting diodes (UVLEDs). The orange-reddish emission of Mn^{2+} in these phosphors can be used as a red component in the tri-color system and may be enhanced by adjusting the Mn^{2+}/Eu^{2+} ratio. The energy transfer from Eu^{2+} to Mn^{2+} is observed with a transfer efficiency of ~0.45 and a critical distance of ~10 Å. The results reveal that $Sr_{2-x-y}P_2O_7$:xEu^{2+},yMn^{2+} phosphors could be used in white light UVLEDs.

Keywords: A. Optical materials; D. Luminescence

1. Introduction

White light ultraviolet light emitting diodes (w-UVLEDs) have attracted much attention recently because of their potential applications for daily lighting needs [1–6]. One of the approaches for making w-UVLEDs is to coat the UVLEDs with tri-color phosphors or single-phase-full-color phosphors [3–6]. Due to the lack of efficient red or single-phase-full-color phosphors suitable for the excitation of the UVLEDs (around 370–400 nm), searching for novel phosphors fitting the requirements of w-UVLED is imperative.

In a commercial phosphor family, most members are oxides due to their stability, high efficiency and easy-preparation. Currently, there are a few ways to acquire UVLED excited red phosphors in oxides. Eu^{3+} in certain hosts [7], such as molybdates, tungstates and borates, has relatively strong f–f excitations at around 390 nm and presents red emissions in the range 610–620 nm. Searching for new UVLED excited red phosphors were conducted by using the generic algorithm-assisted combinatorial chemistry method [2], where a novel red phosphor with the composition $Eu_{0.14}Mg_{0.18}Ca_{0.07}Ba_{0.12}B_{0.17}Si_{0.32}O_{\delta}$ was found. In this phosphor, the Eu^{3+} ions as the activator are located at low symmetric sites and at these sites, the excitation probabilities of Eu^{3+} f–f transitions in the near UV region are relatively strong. However, this kind of phosphors would not be very efficient, because the f–f excitations are

* Corresponding author. Tel.: +86 10 62754188; fax: +86 10 62753541.
E-mail address: xpjing@pku.edu.cn (X.-P. Jing).

0025-5408/$ – see front matter
doi:10.1016/j.materresbull.2007.07.039

intrinsically spin and parity forbidden transitions. In some hosts, Mn^{2+} can give the luminescence from orange to red, thus choosing Mn^{2+} as the activator is another way to design UVLED red phosphors [8]. However, the efficiency of this type of phosphors is not supposed to be very high, because the d–d transitions of Mn^{2+} are also forbidden transitions, and their excitations is not very effective in some hosts. As we know, Eu^{2+} has a high efficiency for both excitation and emission in many hosts, because they arise from the allowed transition between the 5d and 4f levels. Co-doping of the Eu^{2+}–Mn^{2+} pair has recently been adopted as a means to design new red phosphors. Typically, Eu^{2+} can transfer its absorbed energy fully or partially to Mn^{2+}, consequently red (orange-reddish) or single-phase-full-color phosphors can be obtained [4–6,9–11]. The emission of Mn^{2+} varies from green to red, which depends on the strength of its coordination field. Therefore, a suitable coordination field at the Mn^{2+} site is critical to obtain a red emission.

Some Eu^{2+}–Mn^{2+} co-doped phosphors for w-UVLED applications were reported, such as $Ba_3MgSi_2O_8$:Eu^{2+},Mn^{2+} [4], $CaAl_2Si_2O_8$:Eu^{2+},Mn^{2+} [5], and $SrZn_2(PO_4)_2$:Eu^{2+},Mn^{2+} [6]. The patented phosphor, Eu^{2+}–Mn^{2+} co-doped α-$Sr_2P_2O_7$, can generate white light when blended with other phosphors in UVLED [18]. However, no detailed information about this phosphor is available in the literature. In the present work, the luminescence and energy transfer from Eu^{2+} to Mn^{2+} in this phosphor are discussed. This phosphor has a strong excitation efficiency in the near UV region and both Eu^{2+} (blue) and Mn^{2+} (orange-reddish) can give bright emissions, thus it may have potential applications in w-UVLEDs.

2. Experimental

Powder samples were synthesized by solid-state reactions. Starting materials were $SrCO_3$ (A.R.), $(NH_4)_2HPO_4$ (A.R.), Eu_2O_3 (99.99 %) and $MnCO_3$ (A.R.). After being ground thoroughly in stoichiometric ratios by using an agate mortar, the mixed powders were transferred into alumina boats, and then heated in a tube furnace at 1050 °C for 2 h in an Ar atmosphere with 5% H_2. The phase purity was determined by using a powder X-ray diffractometer (XRD, Bruker D8 discover AXS with GADDS). The photoluminescence (PL) excitation and emission spectra of the samples were characterized by using a Hitachi F-4500 fluorescence spectrophotometer, and the integrated areas of the emission peaks were used to represent the PL intensities. The PL decay curves of Eu^{2+} were measured with an FLS920 Combined Steady State and Lifetime Spectrometer (Edinburgh Instrument) with a nanosecond flash lamp as a light source, and those of Mn^{2+} were measured with the Hitachi F-4500 fluorescence spectrophotometer.

3. Results and discussion

3.1. Phase analysis and solid solution ranges

The α-$Sr_2P_2O_7$ phase (a high-temperature phase, $Sr_2P_2O_7$ for short) has an orthorhombic unit cell with space group *Pnma* [12]. In this structure, the two types of PO_4 tetrahedrons are linked to each other by corner sharing and the P_2O_7 groups are isolated by Sr^{2+}. The average bond lengths of P_1–O and P_2–O are 1.541 and 1.542 Å, respectively; the two types of Sr^{2+} sites are both coordinated by nine oxygens with average bond lengths of 2.721 Å for Sr_1–O and 2.679 Å for Sr_2–O, respectively.

The XRD patterns of all the doped samples $Sr_{2-x-y}P_2O_7$:xEu^{2+},yMn^{2+} were recorded. The patterns agreed well with the JCPDS file 24-1011, which indicates that the doped samples synthesized in this work are phase-pure. The solid solution ranges of the system $Sr_{2-x-y}P_2O_7$:xEu^{2+},yMn^{2+} were investigated. Fig. 1 represents the variation of the unit cell volume of $Sr_{2-x-y}P_2O_7$:xEu^{2+},yMn^{2+} with Mn^{2+} content y ($x = 0$). The volume decreases with Mn^{2+} content y when $y < 0.25$, because the ionic radius of Mn^{2+} ($r = 0.83$ Å, CN = 6, Shannon data [17]) is smaller than that of Sr^{2+} ($r = 1.18$ Å, CN = 6). When $y > 0.25$, the volume becomes constant. Therefore, the solid solution range for Mn^{2+} in this system is not beyond $y = 0.25$. The solid solution range for Eu^{2+} in the system is narrow and not wider than $x = 0.04$ ($y = 0$). When x is larger than this value, the impurity phase is clearly evident. The experimental results also indicate that the solid solution range of Eu^{2+} increases slightly with increasing Mn^{2+}content.

3.2. Excitation and emission spectra of Eu^{2+}/Mn^{2+} singly doped and co-doped $Sr_2P_2O_7$

In order to study the luminescence of Eu^{2+}–Mn^{2+} co-doped $Sr_2P_2O_7$, the excitation and emission spectra of the Eu^{2+} or Mn^{2+} singly doped phosphor were investigated and shown in Fig. 2. In Fig. 2(a), the strong emission with peak

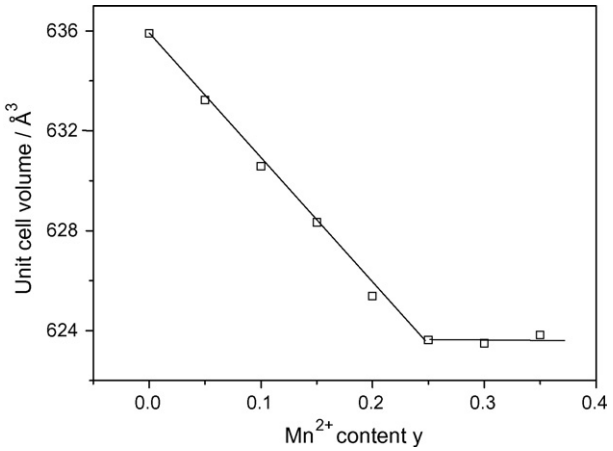

Fig. 1. Dependence of the unit cell volume of the system $Sr_{2-x-y}P_2O_7$:xEu^{2+},yMn^{2+} ($x = 0$) on Mn^{2+} content y.

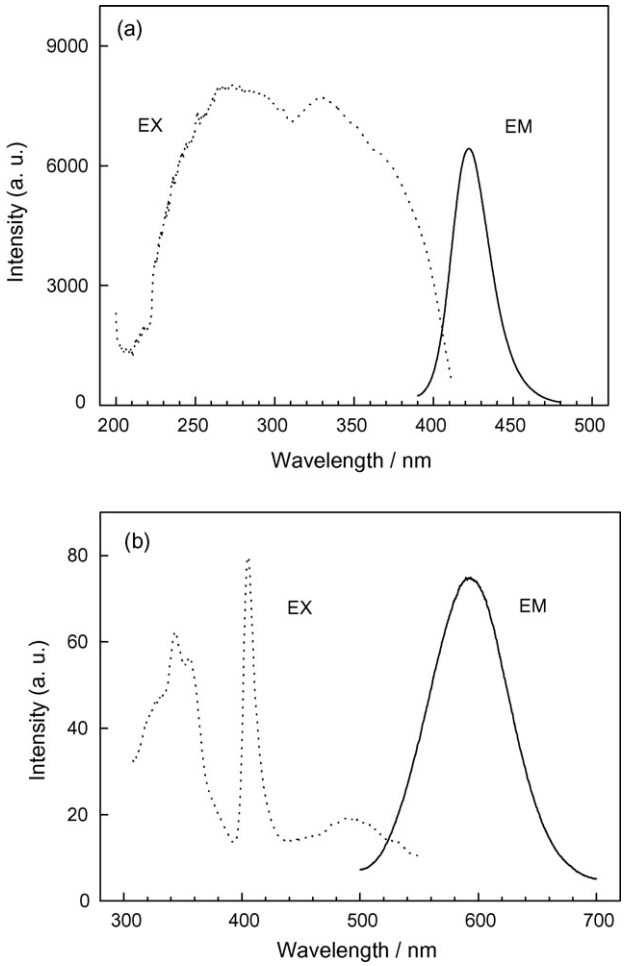

Fig. 2. Excitation (EX) and emission (EM) spectra of (a) $Sr_{1.96}P_2O_7$:$0.04Eu^{2+}$ ($\lambda_{EX} = 380$ nm, $\lambda_{EM} = 420$ nm) and (b) $Sr_{1.85}P_2O_7$:$0.15Mn^{2+}$ ($\lambda_{EX} = 405$ nm, $\lambda_{EM} = 585$ nm).

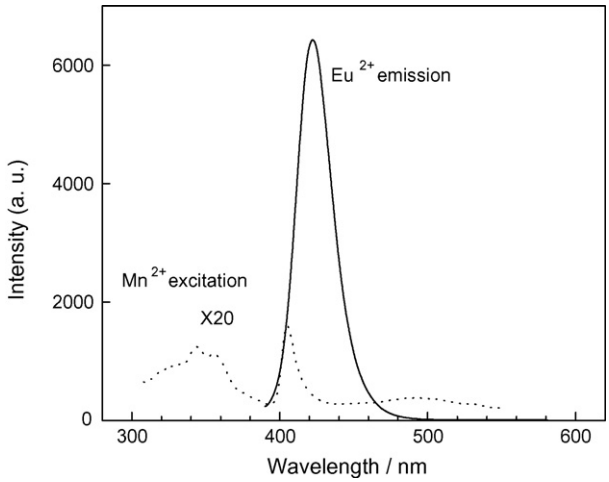

Fig. 3. Spectral overlap between the emission peak of $Sr_{1.96}P_2O_7$:0.04Eu^{2+} (solid line, λ_{EX} = 380 nm) and the excitation peak of $Sr_{1.85}P_2O_7$:0.15Mn^{2+} (dotted line, λ_{EM} = 585 nm).

position at 420 nm is attributed to $4f^65d^1 \rightarrow 4f^7$ transitions of Eu^{2+}. The excitation of Eu^{2+} presents a broad band, which consists of unresolved sub-bands due to the $4f^65d^1$ multiple excited states. In the excitation spectrum of Mn^{2+} in Fig. 2(b), the peaks centered at 340, 355, 405 nm are assigned to the transitions from $^6A_1(^6S)$ to $^4E(^4D)$, $^4T_2(^4D)$ and $[^4A_1(^4G)$, $^4E(^4G)]$ levels, respectively [5]. The emission band centered at 585 nm corresponds to the $^4T_1(^4G) \rightarrow {}^6A_1(^6S)$ transition of Mn^{2+}. Since these transitions are spin and parity forbidden, both the excitation and emission intensities are relatively weak.

Fig. 3 demonstrates the spectral overlap between the emission peak of Eu^{2+} and the excitation peak of Mn^{2+} in each singly doped $Sr_2P_2O_7$. It can be speculated that the energy transfer from Eu^{2+} to Mn^{2+} may occur. Actually, in this work, it was found that the 585 nm emission of Mn^{2+} was effectively sensitized by Eu^{2+}. Fig. 4 shows that the profile of the excitation spectrum for the 585 nm emission of Mn^{2+} is similar to that of Eu^{2+}, which gives proof for the energy transfer from Eu^{2+} to Mn^{2+}. The excitation band of Mn^{2+} in the Eu^{2+}–Mn^{2+} co-doped samples extends from 220 to 430 nm, thus, the phosphors in this system are suitable for w-UVLED applications.

3.3. Influences of Eu^{2+} and Mn^{2+} contents on the PL properties of $Sr_2P_2O_7$:Eu^{2+},Mn^{2+} phosphors

The emission wavelength of Mn^{2+} shifts from 565 to 585 nm with the increase of Mn^{2+} content y in the range of 0.05–0.20, as shown in Fig. 5. The red shift benefits w-UVLED applications, whereas the emission wavelength of

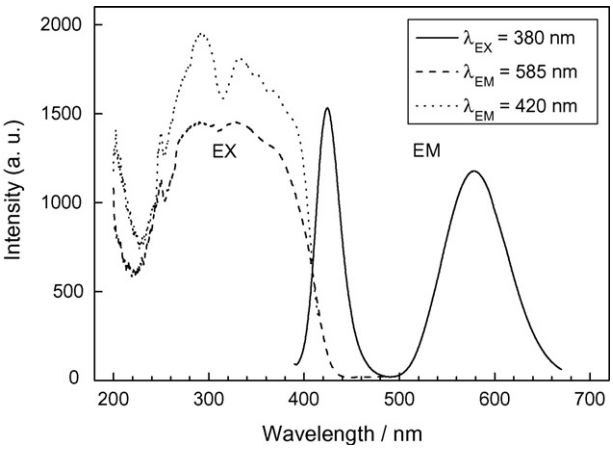

Fig. 4. Excitation (EX) and emission (EM) spectra of $Sr_{1.81}P_2O_7$:0.04Eu^{2+},0.15Mn^{2+}.

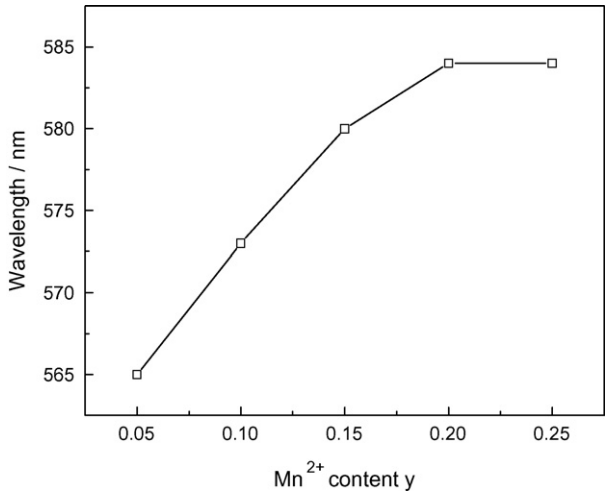

Fig. 5. Wavelength dependence of Mn^{2+} emission on Mn^{2+} content y in the system $Sr_{2-x-y}P_2O_7$:xEu^{2+},yMn^{2+} ($x = 0$).

Eu^{2+} does not change clearly (not shown in the figure). The influences of Eu^{2+} and Mn^{2+} contents on the PL intensities of the $Sr_{2-x-y}P_2O_7$:xEu^{2+},yMn^{2+} system were investigated and the results are illustrated in Fig. 6. The PL intensity of Eu^{2+}, I_{Eu}, decreases dramatically and monotonically with the increase of Mn^{2+} content y, and the intensity of Mn^{2+} emission, I_{Mn}, increases with the increase of Eu^{2+} content x ($x < 0.04$), which further supports the occurrence of the energy transfer from Eu^{2+} to Mn^{2+}. The optimized Mn^{2+} content y for the Mn^{2+} emission is about 0.15, and the optimized Eu^{2+} content x for the Eu^{2+} emission is about 0.01. The variations of the ratios of Mn^{2+} intensity to Eu^{2+}

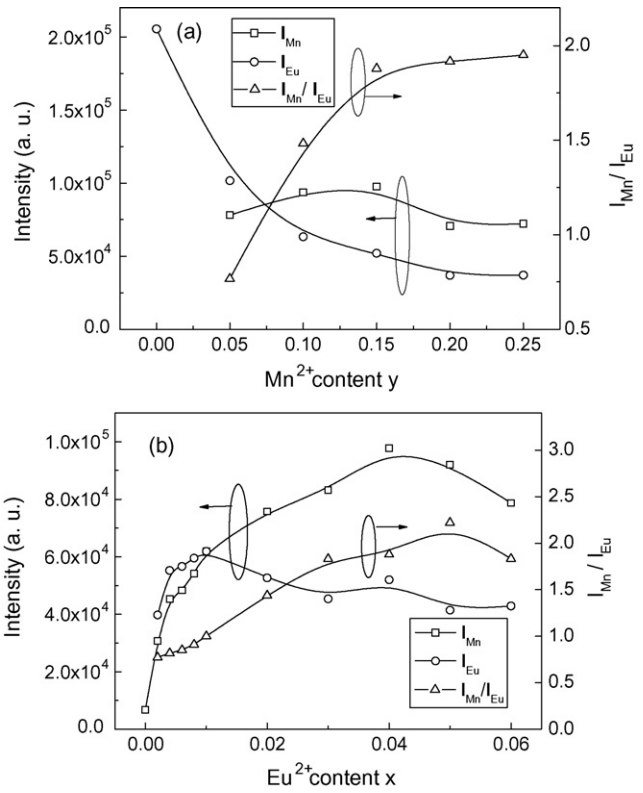

Fig. 6. Dependences of PL intensities of Eu^{2+} and Mn^{2+} emissions and the intensity ratios I_{Mn}/I_{Eu} on Eu^{2+} or Mn^{2+} contents in the systems: (a) $Sr_{1.96-y}P_2O_7$:$0.04Eu^{2+}$,yMn^{2+} and (b) $Sr_{1.85-x}P_2O_7$:xEu^{2+},$0.15Mn^{2+}$.

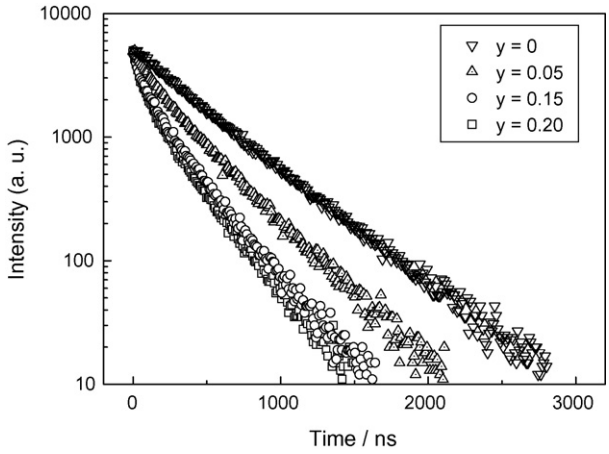

Fig. 7. Selected decay curves of Eu^{2+} emission (420 nm) in the system $Sr_{1.96-y}P_2O_7$:0.04Eu^{2+},yMn^{2+} excited by 380 nm UV light.

intensity, i.e. I_{Mn}/I_{Eu}, with respect to the contents of Eu^{2+} and Mn^{2+} are also represented in Fig. 6. The ratios increase with x and y when $x < 0.05$ and $y < 0.15$, which indicates that the efficiencies of the energy transfer from Eu^{2+} to Mn^{2+} increase in the above ranges. It should be pointed out that although the emission intensity of Eu^{2+} remains strong in all the co-doped samples, the emission intensity of Mn^{2+} can be at least two times stronger than that of Eu^{2+}. This benefits the applications of $Sr_2P_2O_7$:Eu^{2+},Mn^{2+} as the red component in w-UVLEDs.

3.4. Decay curve measurements

The energy transfer from Eu^{2+} to Mn^{2+}, which results in the improvement of Mn^{2+} emission intensity, is strongly evidenced by the decay behavior of the Eu^{2+} emission in co-doped samples. The selected decay curves of Eu^{2+} with the variation of Mn^{2+} content y for the system $Sr_{1.96-y}P_2O_7$:0.04Eu^{2+},yMn^{2+} are illustrated in Fig. 7, and the selected decay curves of Mn^{2+} with the variation of Eu^{2+} content x for the system $Sr_{1.85-x}P_2O_7$:xEu^{2+},0.15Mn^{2+} are illustrated in Fig. 8. The decay curves of both Eu^{2+} and Mn^{2+} can be expressed by an exponential function [13]:

$$I = I_0 \exp\left(-\frac{t}{\tau}\right) \tag{1}$$

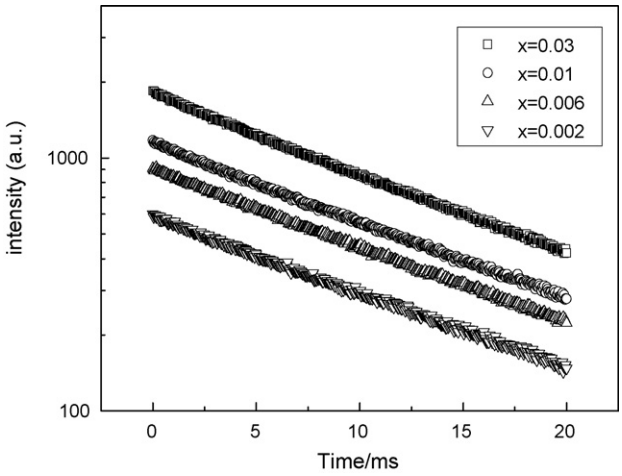

Fig. 8. Selected decay curves of Mn^{2+} emission (585 nm) in the system $Sr_{1.85-x}P_2O_7$:xEu^{2+},0.15Mn^{2+} excited by 380 nm UV light.

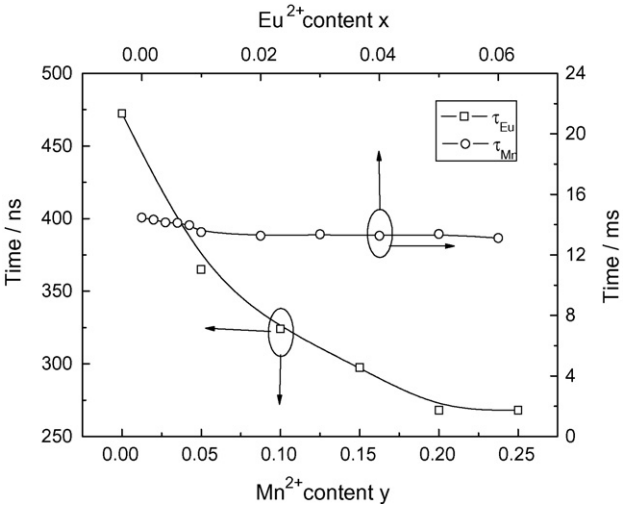

Fig. 9. Dependences of the lifetime of Eu^{2+} emission (τ_{Eu}) on Mn^{2+} content y in the system $Sr_{1.96-y}P_2O_7$:0.04Eu^{2+},yMn^{2+} and the lifetime of Mn^{2+} emission (τ_{Mn}) on Eu^{2+} content x in the system $Sr_{1.85-x}P_2O_7$:xEu^{2+},0.15Mn^{2+}.

where I and I_0 are the luminescent intensities at time t and 0, respectively and τ is the luminescent lifetime which can be calculated from the slopes of the decay curves. The variation of the lifetime of Eu^{2+} emission, τ_{Eu}, with Mn^{2+} content y in the system $Sr_{1.96-y}P_2O_7$:0.04Eu^{2+},yMn^{2+} and the variation of the lifetime of Mn^{2+} emission, τ_{Mn}, with Eu^{2+} content x in the system $Sr_{1.85-x}P_2O_7$:xEu^{2+},0.15Mn^{2+} are shown in Fig. 9. τ_{Eu} declines monotonically from 475 ns to 270 ns with the increase of Mn^{2+} content y, which gives strong evidence for the occurrence of the energy transfer from Eu^{2+} to Mn^{2+}. τ_{Mn} (~13 ms) does not change obviously with Eu^{2+} content x, because τ_{Mn} is longer than τ_{Eu} by about four orders of magnitude. This cannot be dramatically affected by Eu^{2+} content even though the energy transfer occurred.

The energy transfer efficiency (η_T) from Eu^{2+} to Mn^{2+} in the $Sr_{1.96-y}P_2O_7$:0.04Eu^{2+},yMn^{2+} system can be calculated by using the following formula suggested by Paulose et al. [14]:

$$\eta_T = 1 - \frac{\tau_s}{\tau_{s0}} \tag{2}$$

where τ_{s0} is the lifetime of the sensitizer Eu^{2+} in the sample in the absence of Mn^{2+}, and τ_s is the lifetime of Eu^{2+} in the presence of Mn^{2+}. Fig. 10 shows that with the increase of Mn^{2+} content, the transfer efficiency η_T increases gradually. When the Mn^{2+} content y is larger than 0.15, η_T approaches its saturated value of ~0.45. This result is roughly in agreement with the data given in Fig. 6.

The critical distance R_c for the energy transfer from Eu^{2+} to Mn^{2+} was calculated using the concentration quenching method. The average distance R_{Eu-Mn} between Eu^{2+} and Mn^{2+} can be represented by the equation suggested by Blasse [15]:

$$R_{Eu-Mn} = 2\left(\frac{3V}{4\pi xN}\right)^{1/3} \tag{3}$$

where N is the number of molecules in the unit cell, V the unit cell volume and x is the total concentration of Eu^{2+} and Mn^{2+}. If the critical concentration x_c is used in the above equation, R_c can be obtained. The critical concentration x_c is defined as, at which the luminescence intensity of Eu^{2+} reduces to half of that for the sample in the absence of Mn^{2+}. Fig. 6(a) indicates that when the Mn^{2+} content is ~0.05, the Eu^{2+} intensity decreases to half. Accordingly x_c is about 0.04 + 0.05 = 0.09 and the critical distance R_c is estimated by Eq. (3) to be about 14.9 Å.

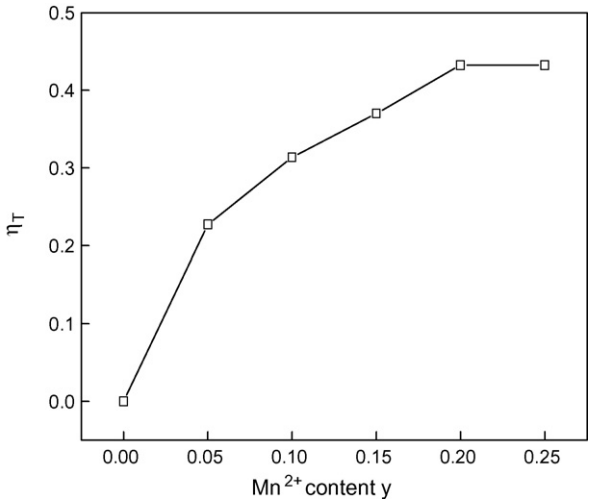

Fig. 10. Dependence of the transfer efficiency η_T on Mn^{2+} content y in the system $Sr_{1.96-y}P_2O_7{:}0.04Eu^{2+},yMn^{2+}$.

We also calculate R_c using the energy transfer mechanism. The energy transfer from Eu^{2+} to Mn^{2+} is considered as a dipole-quadruple mechanism [5,6]. The critical distance R_c can also be represented by [5,15,16]:

$$R_c^8 = 0.63 \times 10^{28} \times \frac{f_q \lambda_s^2 Q_A}{f_d E_S^4} \int F_S(E) F_A(E) dE \quad (4)$$

where $Q_A = 4.8 \times 10^{-16} f_d$, which is the absorption cross-section of Mn^{2+}; $f_d = 10^{-7}$ and $f_q = 10^{-10}$, which are the oscillator strengths of the dipole and quadruple electrical absorption transitions for Mn^{2+}; λ_S (in Å) and E_S (in eV) are the emission wavelength and emission energy of Eu^{2+}. $\int F_S(E)F_A(E)dE$ is the spectral overlap of the Eu^{2+} emission $F_S(E)$ and the Mn^{2+} excitation $F_A(E)$ (the spectra are normalized), which is estimated to be about 9.90 eV^{-1}. Based on the above parameters, R_c is calculated to be about 12.8 Å. These R_c data are larger than that reported in previous work [5,6], thus energy transfer may occur more easily in this host. This is in agreement with the strong emission of Mn^{2+} even at low concentrations of Eu^{2+} and Mn^{2+}.

4. Conclusions

In the present work, the photoluminescence properties of $Sr_{2-x-y}P_2O_7{:}xEu^{2+},yMn^{2+}$ are discussed. The Mn^{2+} in this system can be effectively excited in a wide UV region especially in the near UV range; it gives an intense emission peak at 585 nm, thus the phosphors in this system may be chosen as the red component in the tri-color system and applied in w-UVLEDs. The energy transfer from Eu^{2+} to Mn^{2+} in this system is discussed based on the excitation and emission spectra as well as on the luminescence decay curves, which gives a transfer efficiency of about 0.45 and a critical distance of about 10 Å between Mn^{2+} and Eu^{2+} for this transfer.

Acknowledgments

We are thankful for the financial support from the State Key Program for Basic Research of China (G1998061306) and the National Nature Science Foundation of China (20221101 and 20423005).

References

[1] D.A. Steigerwald, J.C. Bhat, D. Collins, R.M. Fletcher, M. Ochiai Holcomb, M.J. Ludowise, P.S. Martin, S.L. Rudaz, IEEE J. Quantum. Elect. 8 (2002) 310.
[2] K.-S. Sohn, B.I. Kim, N. Shin, J. Electrochem. Soc. 151 (2004) H243.
[3] A.A. Setlur, H.A. Comanzo, A.M. Srivastava, W.W. Beers, J. Electrochem. Soc. 152 (2005) H205.

[4] J.S. Kim, K.T. Lim, Y.S. Jeong, P.E. Jeon, J.C. Choi, H.L. Park, Solid State Commun. 135 (2005) 21.
[5] W.-J. Yang, L. Luo, T.-M. Chen, N.-S. Wang, Chem. Mater. 17 (2005) 3883.
[6] W.-J. Yang, T.-M. Chen, Appl. Phys. Lett. 88 (2006) 101903.
[7] J. Wang, X. Jing, C. Yan, J. Lin, J. Electrochem. Soc. 152 (2005) G186.
[8] T. Murata, T. Tanoue, M. Iwasaki, K. Moringa, T. Hase, J. Lumin. 114 (2005) 207.
[9] U.G. Caldiño, A.F. Muñoz, J.O. Rubio, J. Phys. Condens. Matter 5 (1993) 2195.
[10] A. Mendez, F.L. Ramos, H. Riveros, E. Camarillo, U.G. Caldiño, J. Mater. Sci. Lett. 18 (1999) 399.
[11] G.Q. Yao, J.H. Lin, L. Zhang, G.X. Lu, M.L. Gong, M.Z. Su, J. Mater. Chem. 8 (1998) 585.
[12] Brown, Calvo, J. Solid State Chem. 1 (1970) 173.
[13] G. Blasse, B.C. Grabmarier, Luminescent Materials, Sprinnger-Verlag, Berlin, Germany, 1994, p. 96.
[14] P.I. Paulose, G. Jose, V. Thomas, N.V. Unnikrishnan, M.K.R. Warrier, J. Phys. Chem. Solids 64 (2003) 841.
[15] G. Blasse, Philips Res. Rep. 24 (1969) 131.
[16] D.L. Dexter, J. Chem. Phys. 21 (1953) 836.
[17] R.D. Shannon, Acta Crystallogr. A 32 (1976) 751–767.
[18] A.A. Setlur, A.M. Srivastava, H.A. Comanzo, D.D. Doxsee, US Patent 6,685,852 (2004).